

Effect of Flow Pulses on Degradation Downstream of Hapcheon Dam, South Korea

Young Ho Shin¹ and Pierre Y. Julien, M.ASCE²

Abstract: The changes in channel geometry downstream of Hapcheon Dam, South Korea, are closely examined. Daily pulses of water from peak hydropower generation and from sudden sluice gate operations affect the 45-km reach of the Hwang River between the Hapcheon Reregulation Dam and the Nakdong River. From 1983 to 2003, the median bed-material size, d_{50} , increased from 1.0 to 5.7 mm, and the bed slope of the reach decreased from 94 to 85 cm/km. The vertical riverbed degradation averaged 2.6 m for a distance of 20 km below the reregulation dam. A simple analytical model is developed to predict the increase in sediment transport and the river bed adjustments from flow pulses in comparison with steady flow discharges. Numerical model simulations confirm the theoretical prediction that sediment transport rates from daily pulses are 21% higher than for steady flow discharges. Unsteady sediment transport simulations indicate that the channel bed degradation should extend mostly 20–25 km below the reregulation dam and should not change much after 2013.

DOI: 10.1061/(ASCE)HY.1943-7900.0000287

CE Database subject headings: Channels; Geometry; Dams; Korea, South; Sediment transport.

Author keywords: Alluvial channels; Downstream hydraulic geometry; Dams; Reregulation dams; Flow pulses; Hwang River.

Introduction

Dams affect the downstream hydraulic geometry of rivers through changes in bed elevation, channel width, flow depth, bed-material sizes, armoring, and bank vegetation. The general issues of channel response to changes in water and sediment regimes are discussed in the literature on hydraulic geometry and regime theory (Ferguson 1986; Hey 1979; Huang and Nanson 2000; Lamberti 1992; Miller 1991a,b; Simon and Thorne 1996; Yang 1992). Hydraulic geometry relationships describe channel adjustments either at a cross section (at-a-station) or in the downstream direction, in response to changes in imposed flows and sediment inputs (Phillips et al. 2005). Leon et al. (2009) showed that wider river reaches develop steeper slopes than narrower reaches of the same river.

Dam construction induces river channel adjustments as sediment trapped above the dam results in clearer water immediately downstream of the dam (Downs and Gregory 2004), and also usually reduces the magnitude of flood peaks. For example, Williams and Wolman (1984) showed that flood peaks have been reduced in magnitude as much as 90% at 21 reservoir sites in central and southwestern United States. Page et al. (2005) re-

cently reported on the effects of altered flow regimes on the frequency and duration of bankfull discharge of the Murrumbidgee River in Australia. Flood peaks significantly decreased and bankfull discharge with return periods of 1.25 and 2 years have been reduced by between 29 and 50% after dam completion. A common response to the release of clear water below dams is the degradation of the channel bed, typically at rates much higher than in natural rivers (Knighton 1998). When the sediment load is less than the capacity of the flow, some degradation may occur if the bed material is fine grained (Brandt 2000). Gregory and Park (1974) showed cross section changes downstream of the Clathworthy Reservoir on the River Tone, U.K., after decreased water discharges. Channel capacity was reduced by 54% downstream of the reservoir. Channel changes also include bed degradation and armoring (Williams and Wolman 1984; Simon et al. 2002; Grant et al. 2003). Armoring refers to coarsening of the bed-material size as a result of the degradation of well-graded sediment mixtures (Julien 2002). Channel changes downstream of Cochiti Dam in New Mexico have been recently investigated by Richard and Julien (2005) and Richard et al. (2005).

In South Korea, 20 years have passed since some multipurpose dams were completed, motivating a study of the river changes of the downstream reaches. The Hwang River experienced significant changes and was selected for this analysis. The study reach covers 45 km from the Hapcheon Reregulation Dam to the confluence with the Nakdong River. Field surveys suggest that channel bed degradation, bed-material coarsening, channel narrowing, and vegetation expansion may be in progress downstream of the Hapcheon Reregulation Dam. The basic studies [Ministry of Construction and Transportation (MOCT) of Korea 1983, 1993, 2003] were conducted by the Korean government (MOCT) and a governmental agency [Korea Water Resources Corporation (KOWACO)]. A river basin investigation studied climate and land use changes, and also included river channel surveys and bed-material sampling as part of a broader river channel management plan. The report showed evidence of channel bed degradation and

¹Manager, Korea Water Resources Corporation (K-water), Daejeon, South Korea; formerly, Postdoctorate, Dept. of Civil and Environmental Engineering, Colorado State Univ., Fort Collins, CO 80523. E-mail: yhshin@kwater.or.kr

²Professor, Dept. of Civil and Environmental Engineering, Colorado State Univ., Fort Collins, CO 80523 (corresponding author). E-mail: pierre@engr.colostate.edu

Note. This manuscript was submitted on November 6, 2007; approved on May 20, 2010; published online on December 15, 2010. Discussion period open until June 1, 2011; separate discussions must be submitted for individual papers. This paper is part of the *Journal of Hydraulic Engineering*, Vol. 137, No. 1, January 1, 2011. ©ASCE, ISSN 0733-9429/2011/1-100-111/\$25.00.

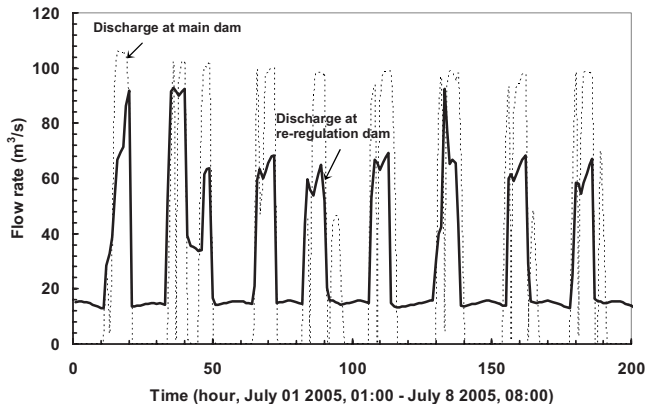


Fig. 1. Typical discharge hydrograph at Hapcheon Dam during flood season from July 1, 2005 to July 8, 2005

bed-material coarsening during the 13-year period immediately after the dam completion. In addition, several researchers investigated the effect of flow regime changes on the river morphology and vegetation cover of the river reach downstream of Hapcheon Dam (Choi et al. 2004; Woo et al. 2004a,b). They analyzed the changes in bed elevation, channel cross sections, and vegetation expansion by this flow regime change, but the effects of the flow pulses by the operation of Hapcheon Reregulation Dam were not considered.

The purpose of the reregulation dam is to dampen discharge fluctuations released below the main power station during peak hydropower generation. Although the reregulation dam attenuates the daily 3-h flow pulses from the main dam, flow pulses still exist during typical floods due to periodical flood gate opening and closing. These daily flow pulses may accelerate the downstream channel changes by increasing sediment transport rate, but the effects need to be quantified. The effects of flow pulses on hydraulic geometry below dams have not been properly investigated in the literature. The data available at Hapcheon dam offer the possibility to quantify the effects of flow pulses compared with steady flow releases. It is also important to predict the future changes in hydraulic geometry and define where and when new equilibrium and stability conditions may be reached. This study aims at a better understanding of river regulation below dams, and the response to varying flow discharges and sediment loads.

This paper focuses on the effect of flow pulses on the changes in downstream hydraulic geometry of alluvial channels. Intuitively, the flow pulses should increase the stream sediment transport capacity, and this effect will be quantified in this paper. The analysis focuses on vertical degradation and is specifically applied to the 45-km reach of the Hwang River between Hapcheon Dam and the confluence with the Nakdong River. After a description of the modeling tools and the study reach, an analysis of the effects of flow pulses is presented, followed by a description of the expected future changes below Hapcheon Reregulation Dam in South Korea.

Modeling Channel Changes

Unsteady flow simulations are considered for this study because of the variability in discharge and attenuating of the flow pulses below the reregulation dam. Fig. 1 shows a typical discharge hydrograph at the Hapcheon Main Dam and reregulation dam during the flood season. Because of the fluctuating nature of the dis-

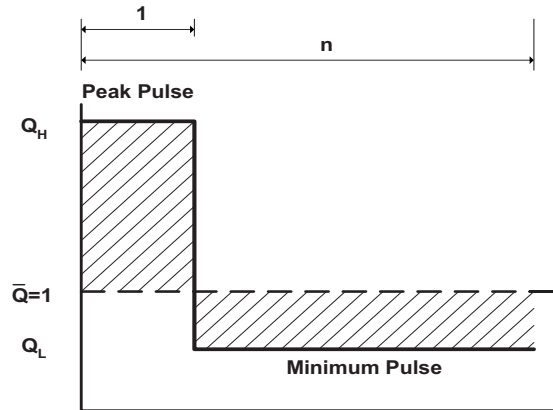


Fig. 2. Diagram of flow pulse

charge on a daily basis, a theoretical analysis of the pulse is first discussed before a description of the numerical model used for the entire reach. The main purpose is to predict future channel changes and evaluate the effect of flow pulses due to the discharge fluctuations from the Hapcheon Dam during flood season and from daily surges in hydropower production. Two methods are considered for this study: (1) the first method applies a simple analytical model to develop an approximate relationship between simplified flow pulse characteristics and the corresponding increase in sediment transport and (2) the second method relies on numerical models for predicting more detailed channel changes and evaluating the effect of flow pulses. Many one-dimensional mathematical models have been developed to simulate water and sediment routing. Models considered for this analysis of steady and unsteady flow simulation below Hapcheon Dam include HEC-6 (U.S. Army Corps of Engineers 1993), FLUVIAL-12 (Chang 2006), CONCEPTS (Langendoen 2000), EFDIC1D (Tetra Tech, Inc. 2001), CCHE1D (Wu and Vieira 2002), GSTARS (Molinas and Yang 1986; Yang and Simões 2000, 2002), and GSTAR-1D [U.S. Department of Interior, Bureau of Reclamation (USBR) 2006].

Analytical Model for Flow Pulse

The following analytical model was developed and applied to obtain a first approximation of the increase in sediment transport caused by flow pulses. A simple rectangular flow pulse is considered as sketched in Fig. 2. The simplified analytical derivation assumes a defined sediment rating curve of the form

$$Q_s = aQ^b \quad (1)$$

where Q_s = sediment discharge (m^3/s) and Q = flow discharge (m^3/s).

The volume of sediment V_s (in m^3) transported during the flow pulse with a time period T is

$$V_s = \int_0^T Q_s dt \quad (2)$$

As sketched in Fig. 2, the flow pulse consists of a period of high flow discharge Q_H of unit duration followed by a period of low flow Q_L during a period of time $n-1$ times as long as the duration of the peak flow pulse. The total pulse duration is T , the period of the flow pulse is n , and the discharge ratio is defined by r as

$$r = Q_H/Q_L \quad (3)$$

where Q_H =peak pulse flow discharge (m^3/s) and Q_L =minimum pulse flow discharge (m^3/s).

The average flow discharge \bar{Q} can then be simply calculated by the following formula:

$$\bar{Q} = Q_L(r + n - 1)/n \quad (4)$$

In the case of steady flow at a constant discharge \bar{Q} over a flow pulse duration T , the sediment volume transported without the flow pulse is

$$\bar{V}_s = a\bar{Q}^b T \quad (5)$$

For the flow pulse shown in Fig. 2, the sediment volume transported with the flow pulse is

$$V_{s \text{ pulse}} = a[(rQ_L)^b + (n-1)Q_L^b]T/n = a(r^b + n - 1)Q_L^b T/n \quad (6)$$

where $V_{s \text{ pulse}}$ =sediment volume transported with the flow pulse.

A sediment pulsing coefficient K_p is defined as the ratio of the sediment volumes transported with and without the flow pulse

$$K_p = V_{s \text{ pulse}}/\bar{V}_s = (r^b + n - 1)n^{b-1}/(r + n - 1)^b \quad (7)$$

The sediment transported by a pulse is K_p times the volume of sediment transported under steady flow. Hence, the pulsating nature of the flow can be considered like the case of steady flow with consideration of the sediment pulsing coefficient K_p defined in Eq. (7). It is noticed from Eq. (7) that when $b > 1$, the sediment pulsing coefficient is always greater than 1. This means that flow pulses always increase the sediment transport capacity over that of steady flow. As an example, if the daily flow pulses last 4 h, $n=6$, and the ratio of high to low flows is $r=10$, the coefficient K_p for $b=1.5$ would be 1.54 from Eq. (7). This means that the sediment transport capacity of pulsing flows would be approximately 50% greater than the sediment transport of the same volume of water under steady flow.

Ephemeral flow pulses can also be considered as rivers can possibly dry out during part of the year and the minimum pulse flow thus reduces to zero. In this case of ephemeral flow pulses, the sediment pulsing coefficient K_p asymptotically approaches $K_p = n^{b-1}$ when $r \rightarrow \infty$. The sediment pulsing coefficient for ephemeral flow pulses is always greater than 1 when $b > 1$.

Numerical Model for Bed Elevation Changes

GSTAR-1D was selected for this study reach as it is suited for the simulation of bed elevation changes below the dam after construction. The model has been verified using experimental and field data by Greimann and Huang (2006) and Huang et al. (2006). GSTAR-1D is a one-dimensional hydraulic and sediment transport numerical model developed by the U.S. Bureau of Reclamation (USBR 2006). It can simulate water surface profiles in single channels, dendritic, and looped network channels. It has also both steady and unsteady flow model capability and uses the standard step method to solve the energy equation for steady gradually varied flows. It can solve the Saint-Venant equations for unsteady rapidly varied flows. For simulation of sediment transport, GSTAR-1D uses two methods. For a long-term simulation, the unsteady terms of the sediment transport continuity equation are ignored, and the nonequilibrium sediment transport method is used. For a short-term simulations, the governing equa-

tion for sediment transport is the convection diffusion equation with a source term arising from sediment erosion/deposition (Huang et al. 2006).

GSTAR-1D has limitations (Huang and Greimann 2006), pertaining to its one-dimensional formulation. It should not be applied to situations where a two-dimensional or three-dimensional model is required for detailed simulations of local hydraulic conditions. It ignores secondary currents, lateral diffusion, and super elevation in bends. Input data to GSTAR-1D include cross section data, river length, slope, river network configuration, movable bed definition, Manning's roughness coefficient, discharge and water surface elevation at the upstream or downstream end, and bed-material gradation. The output of GSTAR-1D are water surface elevations, cross section elevation changes due to erosion or deposition, changes to riverbed material, sediment concentrations and sediment load, and bed shear stress.

Study Reach and Available Data

Six multipurpose dams have been constructed in the Nakdong River basin since 1970. These dams provide flood control, water supply, and hydroelectric power generation. The Hapcheon Main Dam, constructed in the narrow canyon of the Hwang River in 1989, and located about 16 km west of Hapcheon City, Korea, serves several purposes including flood control, peak hydropower generation, and water supply. It has a reservoir storage capacity of $790 \times 10^6 m^3$. In addition, a reregulation dam located 6.5 km downstream of the main dam regulates the discharge from the main hydropower station. The main power station is located 2 km upstream from the reregulation dam and operates only 3–8 h per day, except during flood season. The Hwang River flows east to the Nakdong River as shown in Fig. 3. The total river length is 107.6 km and the drainage area covers 1,329 km^2 . The study reach downstream of Hapcheon Dam is 45 km long, with a sub-basin area of 327.4 km^2 . The maximum discharge of the main power station is 119 m^3/s and the reregulation dam regulates this 3-h discharge to approximately 15 m^3/s on a daily basis. Fig. 4 shows a plan view of the Hapcheon Main Dam and the Reregulation Dam. Table 1 provides detailed configuration of the Hapcheon Main Dam and Reregulation Dam.

Most of the data collection on the Hwang River began in 1983 with the national river channel maintenance plan to protect properties from flood damage by the Ministry of Construction of Korea, which is since 1996 known as the MOCT with the purpose to reduce flood damage. Data are generally collected every 10 years and focused on maintenance and construction of levee along the channel especially downstream of the Hapcheon Reregulation Dam. Available data included cross section surveys, bed-material size surveys, flow discharge, meteorological data, water quality, and environmental conditions such as distribution of animals and plants. There are three major data sets for this study reach (1983, 1993, and 2003). The study reach was subdivided into three sub-reaches as shown in Fig. 5. The locations along the channel are measured with reference to the confluence with the Nakdong River.

Discharge Records

Discharge data were gathered from the MOCT and KOWACO gauging stations (from 1969 to 2005). Daily discharge data along the study reach were available from 1969 to present at both gauging stations. The flow discharge data were collected at the

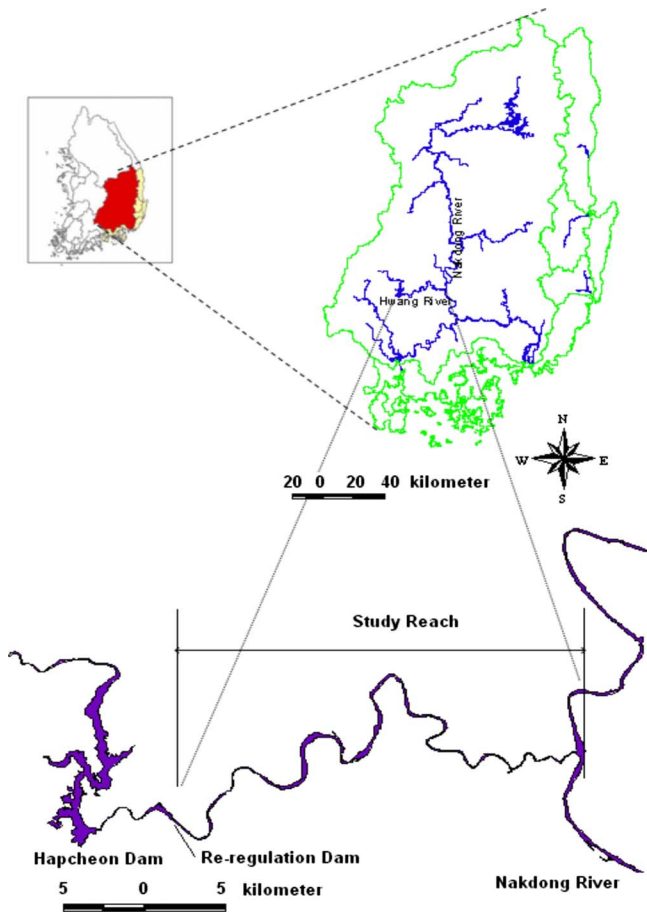


Fig. 3. Study reach of the Hwang River below Hapcheon reregulation dam

Changri Station, which changed its name to the Hapcheon Re-regulation Dam gauging station operated by KOWACO after 1989 (after the dam completion). In addition, hourly and 30-min data are available since 1996. There are two water level gauging stations downstream of the Hapcheon Reregulation Dam, Hapcheon and Jukgo gauging stations operated by MOCT since 1962.

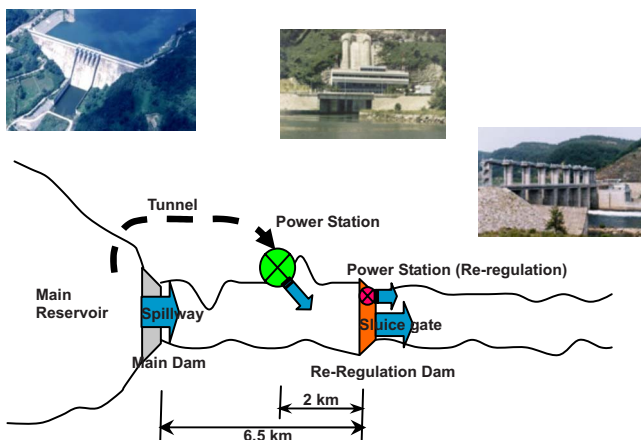


Fig. 4. Plan view of the Hapcheon main dam and reregulation dam

Table 1. Configuration of the Hapcheon Main Dam and Reregulation Dam

Configuration	
1. General	
Location:	Hwang River (tributary of the Nakdong River in Korea)
Catchment area:	925 km ²
Annual mean inflow:	911.4 million m ³
2. Main dam	
Height:	96 m
Length:	472 m
Dam crest elevation:	EL.181.0 m
Type:	concrete gravity dam
3. Reregulation dam	
Height:	29 m
Length:	275.5 m
Type:	concrete and rockfill dam
Location:	6.5 km downstream of the main dam
4. Reservoir of main dam	
Flood water level:	EL.179.0 m
Gross storage capacity:	790 million m ³
Flood control capacity:	80 million m ³
Reservoir area:	25.0 km ²
5. Power generation (main dam)	
Installed capacity:	101,000 kW
Maximum turbine discharge:	119 m ³ /s
Rated head:	95.0 m
6. Power generation (reregulation dam)	
Installed capacity:	1,200 kW
Maximum turbine discharge:	20 m ³ /s
Rated head:	7.3 m
7. Water supply	
Annual water supply:	599 million m ³
Irrigation:	32 million m ³
Municipal and industrial:	520 million m ³
Environmental flow:	47 million m ³

Aerial Photos

Aerial photos are available for 1982, 1993, and 2004 (Fig. 5). The aerial photos were obtained from the National Geographic Information Institute to quantify and compare the adjustment before and after dam construction. These photos have been georeferenced to quantify and identify the location of the active channel width, area, vegetated islands, and numerous other important features. These aerial photos were digitized using the digital elevation model by ERDAS IMAGINE software to get *x-y* coordinates to determine location site and measure lengths and areas. After processing, the images, the active channel area, cross section survey lines, vegetated area, and island area were superposed to the aerial photos by using ArcView 3.2 software.

Cross Section Surveys

Cross section survey data were measured in 1983, 1993, and 2003 for this study reach. The cross section survey data set from 1983

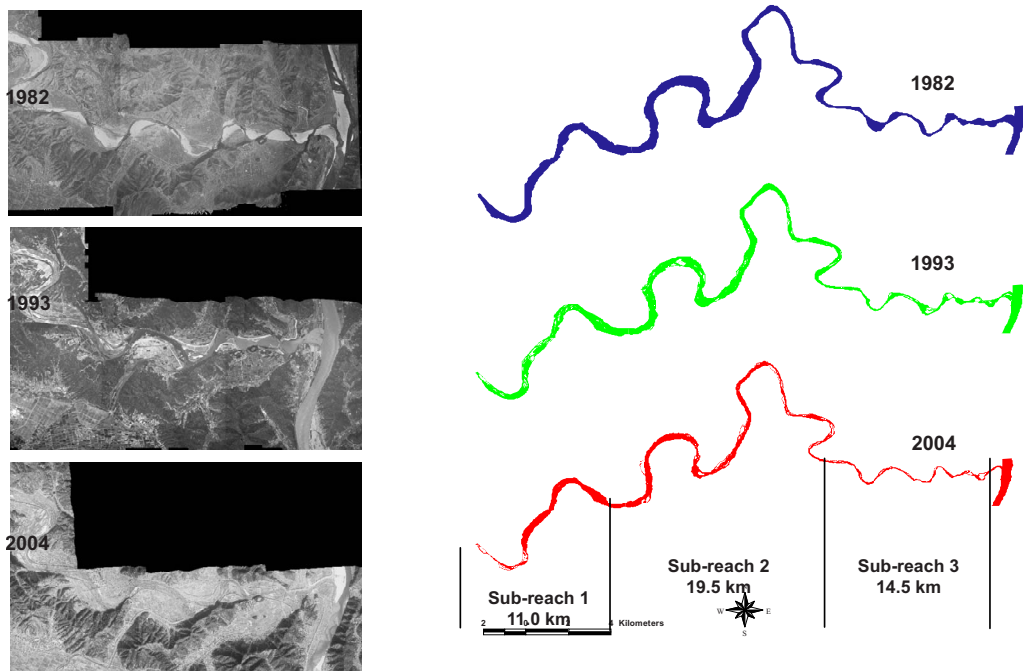


Fig. 5. Aerial photos of Subreach 3 and nonvegetated active channel planform maps of the study reach for 1982–2004

was obtained from the National Water Management Information System of Korea Web site. The cross section survey data sets from 1993, were only available in a survey report, and thus only thalweg elevation data were available in digital form. Finally, the cross section survey data sets from 2003 contained HEC-RAS geometric input file (MOCT of Korea 2003) and were directly used in this study. The cross section surveys were collected approximately 500 m apart for a total of 100 cross sections in 1983 and 1993. However, in 2003, the cross section surveys were collected 250 m apart, with a total of 210 cross sections. Resistance to flow was determined using Manning's n for the entire reach. The calibration showed that n decreased in the downstream direction from 0.035 below the dam to 0.025 near the confluence with the Nakdong River. The Manning's n values reflect the gradual decrease in grain size of the bed material in the downstream direction for the study reach. More details on Manning's n and the calibration run can be found in Shin (2007).

Sediment Transport and Bed Material

Bed material samples were collected at the same time as cross section surveys by MOCT of Korea (1983, 1993, 2003). Sampling was conducted at 13 cross sections in 1983, 46 cross sections in 1993, and 25 cross sections in 2003. Suspended sediment sampling was performed at the Changri gauging station (the Hapcheon Dam site) in 1969 and 1970 to provide sufficient data for the construction of the Hapcheon Dam by Food and Agriculture

Organization of the United Nations (FAO) and KOWACO (1971). The estimated total sediment loads from these suspended sediment data were 1,478 and 477 thousand tons per year in 1969 and 1970, respectively.

A survey of the reservoir sediment deposition of the Hapcheon Main Dam was conducted in 2002 by KOWACO (2002) to evaluate the change of the reservoir storage volume. As a result, the estimated sediment volume was 8,279,000 m³ for a 14-year period (1989–2002). Therefore, the total sediment load was estimated as 946,000 t/year at the Hapcheon Main Dam site (basin area is 925 km²). From this result, we can estimate the total sediment load at the confluence with the Nakdong River as 381,000 t/year. Also, we estimated the sediment transport rates using sediment transport formulas and compared with measured data from the survey of reservoir sediment deposition of the Hapcheon Main Dam in 2002 (KOWACO 2002). The total sediment load estimates from the formulas of Engelund and Hansen (1972), Ackers and White (1973), Yang (1973, 1979), and van Rijn (1984) at the confluence with the Nakdong River are listed in Table 2. The estimated total sediment load was 440,000 t/year by Yang's (1973) method which was selected for estimation of sediment transport in this study reach because it showed the closest value in comparison with field measurements. The estimated sediment-discharge relationship used in this study was therefore $Q_s = 9.77Q^{1.49}$ with both Q and Q_s in m³/s. The value of $b = 1.49$ can

Table 2. Estimated Total Sediment Load at the Confluence with the Nakdong River (1,000 t/year)

Unit	Survey (KOWACO 2002)	Engelund and Hansen (1972)	Ackers and White (1973)	Yang (1973)	Yang (1979)	van Rijn (1984)
10 ³ t/year	381	673	1,194	440	541	1,268
t/km ² /year	1,022	1,806	3,207	1,181	1,452	3,405
m ³ /km ² /year	639	1,129	2,004	738	908	2,128

Note: Survey: estimated from survey result of reservoir sediment deposition of the Hapcheon Dam.

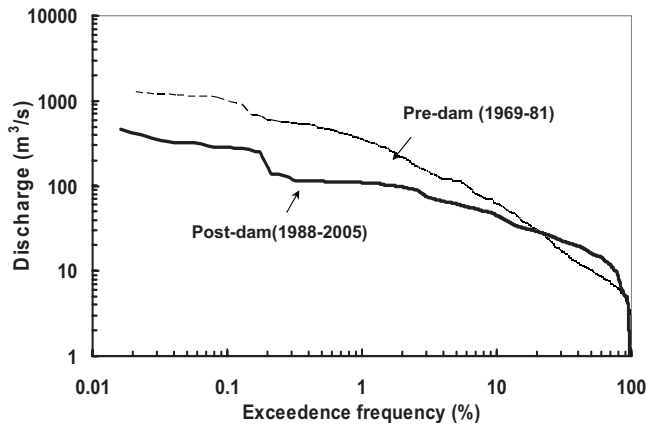


Fig. 6. Flow duration curves at the Hapcheon reregulation dam site from 1969 to 2005

thus be used as a first approximation of the rating curve for the calculation of the sediment pulsing coefficient defined in Eq. (7) for the Hwang River.

Measured Channel Changes

The field measurements of this study reach were used to quantify and analyze channel changes. The water discharge, bed material, bed slope, and channel width were quantified and analyzed to identify historic trends. Water discharge records since 1969 reveal a decline in annual peak discharge after the Hapcheon Main Dam and Reregulation Dam construction. The impact of both Hapcheon Main Dam and the Reregulation Dam on the annual water discharge regime were examined. The dam attenuated mean annual peak discharges greater than $528 \text{ m}^3/\text{s}$ (from 654.7 to $126.3 \text{ m}^3/\text{s}$). The mean annual peak discharge of the postdam period (1989–2005) was only 19% of the predam period (1969–1981). The mean daily discharge was also greater during the predam period than during the postdam period ($28.7 \text{ m}^3/\text{s}$ during predam and $22.1 \text{ m}^3/\text{s}$ during postdam period). The decrease rate was 23% at the Hapcheon Reregulation Dam gauge.

The bankfull discharge (1.58-year discharge frequency) was estimated by using annual daily peak discharges for both the predam (1969–1981) and postdam (1989–2005) periods. The bankfull discharge decreased from $510 \text{ m}^3/\text{s}$ for the predam compared to $86.3 \text{ m}^3/\text{s}$ for the postdam period. From the flow duration curves in Fig. 6, the peak discharges decreased and low discharge increased. The bed material of the study reach changed following construction of the Hapcheon Main Dam and Reregulation Dam. Prior to the dam construction, the channel bed was somewhat coarser in Subreach 1 than the downstream reaches. The median bed-material size, d_{50} , of the entire study reach was 1.07 mm in 1983, but the riverbed coarsened to gravel size following dam construction, especially in the 2-km reach immediately below the reregulation dam. Armoring of the channel bed is noticeable in this reach.

Overall, the bed slope of the entire reach declined from 94 cm/km in 1983 to 85 cm/km in 2003. During the postdam period, the largest degradational changes occurred along the 15-km reach below the reregulation dam. An average degradation of 2.6 m was observed during 1983–2003 periods.

Channel width changes were measured in terms of the nonvegetated active channel digitized from aerial photos taken in 1982,

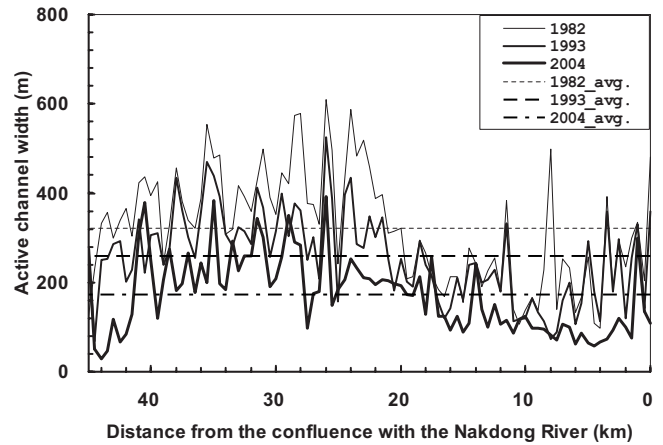


Fig. 7. Nonvegetated active channel widths of the study reach in 1982, 1993, and 2004

1993, and 2004. All subreaches exhibited a decrease in channel width with time since 1982. Subreach 3 exhibited the greatest change with a 53% decrease between 1982 and 2004. Subreach 2 was the widest reach for the entire time period, and the channel width decreased to only 54% of the width in 1982. Overall, the active channel width decreased after the dam construction along the entire study reach from 321 m in 1982 to 172 m in 2004 (Fig. 7). The rate of change in channel width between 1993 and 2004 was faster than between 1982 and 1993.

The width/depth ratios also decreased in most of the reaches except Subreach 3. The width/depth ratio of the entire reach decreased from 279 to 258 from 1982 to 2004, respectively. The sinuosity of all reaches slightly decreased after the dam construction. Also, the total sinuosity of the study reach remained over 1.8 from 1982 to 2004. Subreach 2 was the most sinuous reach among the three subreaches. According to the planform maps of the nonvegetated active channel (see Fig. 5), the planform geometry was relatively unchanged from pre- to postdam period.

According to the field investigation and aerial photos, the channel scour and narrowing has occurred at most of the cross sections along the study reach. The reach immediately below the dam showed the most scour. In the middle reach, approximately between 38 and 15 km, the channel bed reached relatively stable conditions after bed scour and channel narrowing. However, the lower reach showed channel division into several subchannels and island formation with establishment of perennial vegetation such as willow following dam completion. The total active channel area for the entire reach declined over the 20 years.

Model Results

The simulation results are based on the measured cross section, and the daily flow data at Hapcheon Reregulation Dam. According to Williams and Wolman (1984), large reservoirs trap more than 99% of the incoming sediment load, and so the model assumed a clear-water release as upstream boundary at the reregulation dam. The study reach ends at the confluence with the Nakdong River, where water surface elevations were measured. The model consists of 210 cross sections starting at the reregulation dam and ending at the confluence with the Nakdong River.

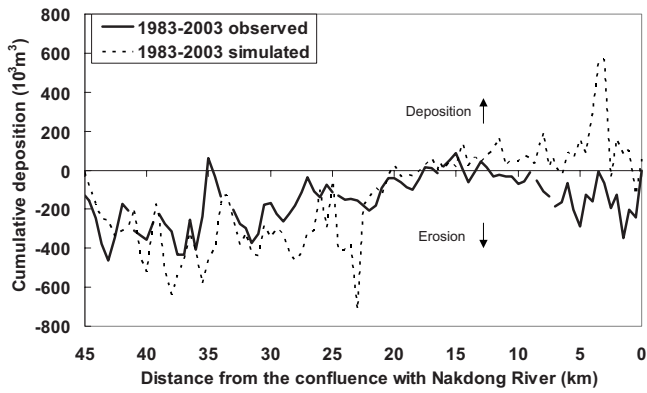


Fig. 8. Measured and predicted cumulative total volume of sediment from 1983 to 2003

Numerical Model Calibration 1983–2003

The GSTAR-1D model was first calibrated using the steady flow conditions and by applying a bankfull discharge of $509.8 \text{ m}^3/\text{s}$ for the predam period (1983–1988) and $86.3 \text{ m}^3/\text{s}$ for the postdam period (1989–2003). A discharge rating curve from the Korea Hydrological Survey Annual Report was used for the downstream boundary condition. The time step for the simulation was 1 h in this case. In the unsteady model described below, the time step was then reduced to 0.01 h or 36 s. The reason for applying the steady flow condition for the 20-year simulation is that the unsteady flow model at a time step of 0.01 h would require too much data and calculation time. The steady flow condition also serves as the base level for the comparison with the unsteady flow model described in the forthcoming section of the paper.

The steady flow condition could easily be used for model calibration. The numerical model produces the cumulative erosion and deposition in the main channel (Fig. 8). The measured cumulative volume was determined by comparing the change in the cross sections of 1983 and 2003, for each cross section. A minus values indicate erosion and plus values indicate deposition. From the reregulation dam to about 18 km from the confluence with the Nakdong River (27 km downstream of the reregulation dam), the field measurements show that the main channel experienced erosion. The differences between the observed and simulated values in the lower reach are due to dredging. The dredged depths exceeded 10 m in the reach between 5 and 2.5 km. Fig. 9 shows the

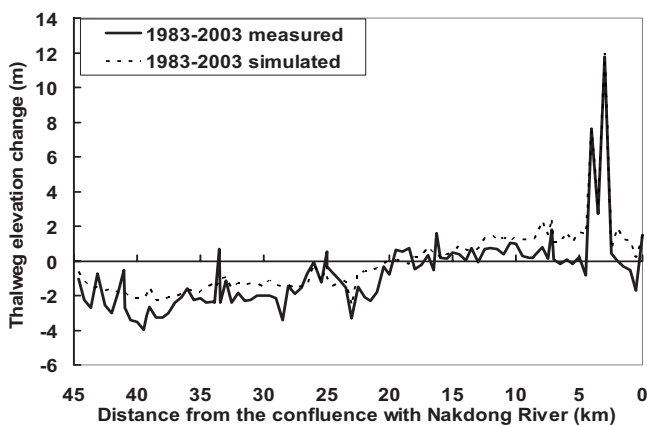


Fig. 9. Measured and predicted thalweg elevation changes from 1983 to 2003

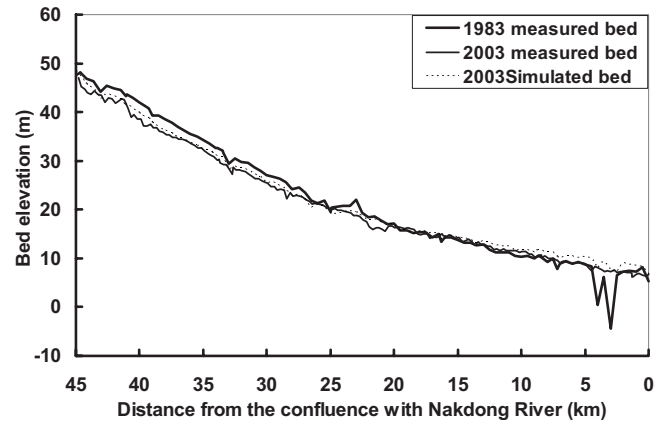


Fig. 10. Measured and predicted thalweg elevations from 1983 to 2003

measured and predicted thalweg elevation changes from the original thalweg elevation measured in 1983. The results of the reach-averaged RMS error analysis of the predicted versus measured thalweg elevation changes is 0.93 m.

Fig. 10 shows measured and predicted thalweg elevation profiles along the study reach. Overall, the model reproduces the thalweg elevation change with similar patterns. However, the simulated thalweg elevation is slightly under estimated (less degradation) compared with measured thalweg elevation from 45- and 20-km reach from the confluence with the Nakdong River and it is a little over estimated (more aggradation) compared with measured thalweg elevation from 20 and 0 km.

Numerical Model Prediction from 2003–2023

After GSTAR-1D model calibration, the parameters were left unchanged for a model application in a predictive mode for the period from 2003 to 2023. In addition, the model used the 2003 measured cross section data, bed gradation, and the average discharge data of the postdam period ($86.3 \text{ m}^3/\text{s}$). The predictive discharge data were replicated from the historical record at the reregulation dam after the dam construction from 1989 to 2005. It is hypothesized that the discharge for the next 20 years (2003–2023) will follow the same pattern and values as shown from the previous recorded discharge (1989–2003) at the reregulation dam.

Fig. 11 shows the measured thalweg elevations in 1983, 2003,

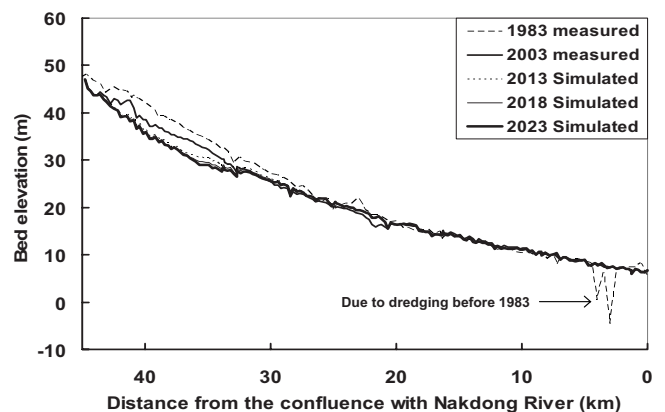


Fig. 11. Measured (1983 and 2003) and predicted thalweg elevation changes from 2003 to 2023 for 20 years

Table 3. Cases of Unsteady Simulation

Case	Flood type	Period	Type of inflow hydrograph	Maximum discharge (m ³ /s)	Minimum discharge (m ³ /s)
1	Typical	July 2, 2005 7:00 a.m.–	Daily pulse	92.9	13.2
2		July 6, 2005 10:00 a.m.	Daily average	33.0	33.0
3	Extreme	August 30, 2002 1:00 a.m.–	Flood peak	504.0	74.9
4		September 3, 2002 4:00 a.m.	Flood average	275.1	275.1

and predicted for 2013, 2018, and 2023. The channel eroded in the 45- to 25-km reach after 1983. The predicted thalweg elevations are not expected to change significantly after 2013. There were very few observable changes in the thalweg elevations from 2013 to 2023.

Flow Pulse Results from the Numerical Model

To evaluate the effect of flow pulses on the downstream channel, four cases are considered: daily pulse (Case 1), daily average (Case 2), flood peak (Case 3), and flood average (Case 4). The discharge hydrographs were applied for unsteady simulation for 100 h along the study reach. The simulation results for the four unsteady flow conditions from GSTAR-1D are presented in Table 3 and Fig. 12.

The model results in Table 4 showed that the sediment transport rate (t/day) due to the daily pulse (Case 1) is 21% bigger than the sediment load determined by the daily average (Case 2). Similarly, the sediment transport rate (t/day) due to the flood peak (Case 3) is 15% larger than the flood average (Case 4). Fig. 13 showed the difference in the cumulative sediment loads (t) from the daily pulse (Case 1) minus the daily average (Case 2). A positive value suggests that the cumulative sediment loads determined by the daily pulse are larger than for the daily average and vice versa for the negative values. From this result, the daily pulse (Case 1) below the reregulation dam affected the entire study reach because the sediment volume of daily pulse (Case 1) is larger than the sediment volume of daily average (Case 2) along the study reach. This analysis in Fig. 13(a) also shows that the effects of daily pulses are uniformly distributed over the 45-km reach.

In the same manner, the differences of the cumulative sediment loads (t) of the flood peak (Case 3) minus the flood average (Case 4) are shown in Fig. 13(b). The values are larger than zero

along most of the study reach, especially downstream the dam between 45 and 25 km, but the values are less than zero near the confluence with the Nakdong River from 10 to 0 km. The results in Fig. 13(b) show that the effects of flood peaks on sediment transport are more pronounced in the 20-km reach immediately below the dam, which is corroborated by the field measurements.

Flow Pulse Results from the Analytical Model

To estimate the effect of flow pulses on sediment transport, the factor K_p is calculated using Eq. (7) as follows. For the Hwang River study reach, $b=1.49$ from the estimated sediment rating curve, $n=3$ (period of pulse is 8 h daily), and the peak and low discharges from Fig. 12 are, respectively, $Q_H=64.4$ m³/s, $Q_L=14.4$ m³/s, thus giving $r=Q_H/Q_L=4.47$.

This corresponds to a value of $K_p=\nabla_s \text{ pulse} / \nabla_s \approx 1.20$ from Eq. (7). This means that the sediment transport capacity from the flow is expected to be approximately 20% larger than the sediment transport rate of the average pulse flow. This 20% increase in sediment transport capacity from the analytical model is similar to the 21% increase calculated from the GSTAR-1D model for Case 1 and Case 2, as shown in Table 4.

Also, the general relationships for K_p as a function of b and n are developed by using Eq. (7) and are shown in Fig. 14. In Fig. 14(a), the value of K_p is plotted for $n=3$ at different values of the discharge ratio and the exponent of the sediment rating curve. It is observed that the coefficient $K_p > 1.1$ only becomes significant when the exponent of the rating curve is greater than 1.25 and when the discharge ratio r is larger than 5. Fig. 14(b) also shows different values of K_p when the exponent of the rating curve $b=1.5$. The results are then quite interesting in that the relative duration of the low and high pulse then becomes far less important than the discharge ratio. The value of $K_p > 1.1$ are then

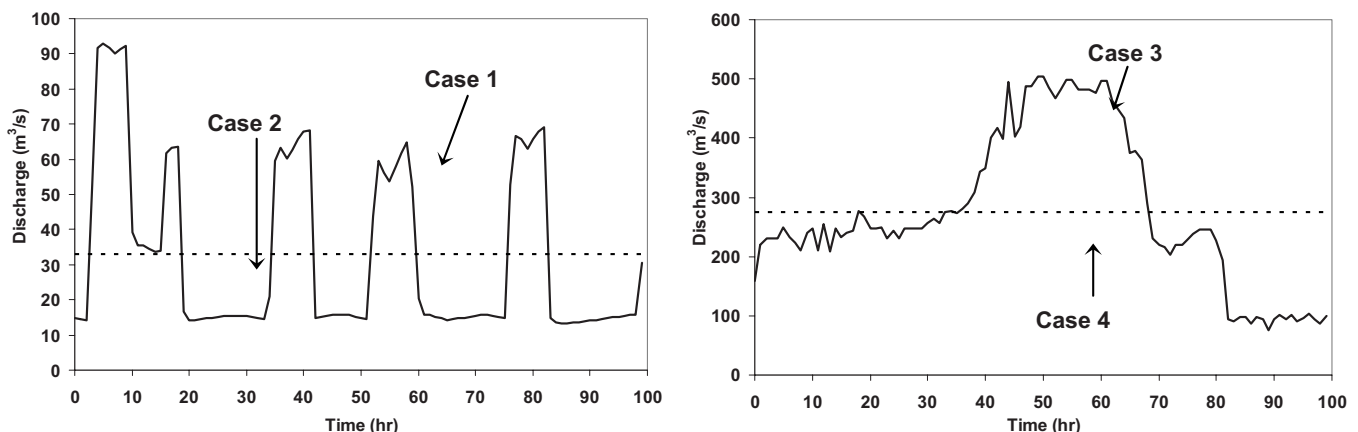
**Fig. 12.** Input hourly discharge hydrographs for four unsteady simulations

Table 4. Simulated and Measured Sediment Transport Rate (t/day) for the Four Cases

	Sediment transport rate (t/day)			
	Case 1	Case 2	Case 3	Case 4
Simulated	1,594 (121% of Case 2)	1,316	11,876 (115% of Case 4)	10,331

observed when the discharge ratio is greater than 3. In summary, this graph is quite instructive and a discharge ratio of about 3 is required for the unsteady flow to increase the sediment discharge by more than 10% compared to the steady flow case.

Discussion of the Results

Limitations of the Model Results

It is perhaps important to first discuss some of the limitations of the numerical model results. This numerical analysis of the channel changes used a constant channel width for the long-term simulations of the vertical degradation changes and riverbed armoring. The recent analysis of Leon et al. (2009) showed that channel narrowing over time in alluvial river reaches would result in flatter slopes. Their Eq. (6) showed that the slope ratio is proportional to the width ratio to the power 1/7. According to their formula, a 50% decrease in channel width would result to a slope that is 90% of the original slope. It is interesting to notice that this exactly replicates the channel slope reduction from 94 to 85 cm/km observed in the Hwang River below Hapcheon Dam. The GSTARS model has been here applied at channel widths that varied in the downstream direction but remained constant in time. It may be interesting in future research to carry out long-term simulations of riverbed degradation below dams with channel widths changing both in space and time.

Future modeling results may also expand upon the comparison of steady versus unsteady flow model performance. There is no doubt that 20+ year simulations of hourly unsteady flow in alluvial channels pose challenges in data availability as well as computing limitations. Our conclusions are based on a relatively limited comparison of steady versus unsteady model results. Future improvements in the comparative performance of steady versus unsteady models should yield interesting results.

One inherent model limitation for unsteady flow simulations is the limited knowledge of sediment transport under unsteady flow. The analysis presented in this paper assumes the existence of a single sediment rating curve. A more complete analysis of the effects of flow pulses should eventually incorporate the loop-rating effect of sediment rating curves.

Nevertheless, these limitations do not overshadow the results presented in this paper. Indeed, it is viewed that the results presented in Fig. 14 should be quite helpful in engineering practice. It is clear that when the difference between the sediment transport rates of flow pulses is less than 10% greater than that of steady flow, the use of steady flow models should be sufficiently accurate for engineering applications. In the case of the Hwang River, the difference is already of the order of 20% and additional research on unsteady flow calculations becomes increasingly interesting.

Morphological Observations

The morphological observations on the measurable channel changes relate very well to the expected results from Lane's (1955) relationship. The results of the channel changes such as the median bed-material size (d_{50}), slope reduction are a result of the Lane relationship given the primary effect of the dam in reducing the sediment discharge downstream of the dam. In this case study, the system degraded because the dam impact on holding so much sediment resulted in channel incision downstream of the dam.

From the incision of longitudinal profile with an average of 2.6 m over a 20-year period, this study reach can also be characterized by the Schumm's channel evolution model (CEM) (Schumm 1985). The channel reaches below Hapcheon Dam have changed from Stages I to III. It will be interesting to monitor in the future whether the system will eventually adjust to Stage III, IV, or V. If later stages of the CEM exist, such as a Stage V, which means the system would eventually tend toward another dynamic equilibrium. Immediately below the dam, it has become clear that the net degradation trend combined with coarsening of the bed-material results in riverbed armoring which would remain stable for a wide range of flow conditions except at very high flows where the bed can be remobilized.

The gravel-bed stream below the dam also results in a different aquatic habitat favoring clear-water fish species. Comparatively, the lower reach closer to the Nakdong River has remained a sand-

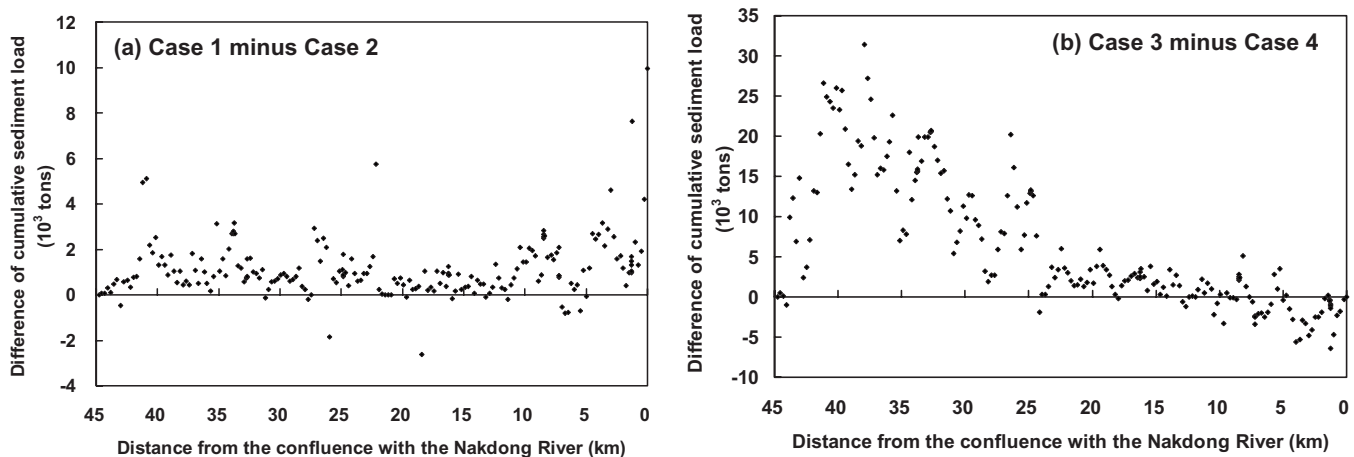


Fig. 13. Difference of cumulative sediment load (10^3 t): (a) Case 1 minus Case 2; (b) Case 3 minus Case 4

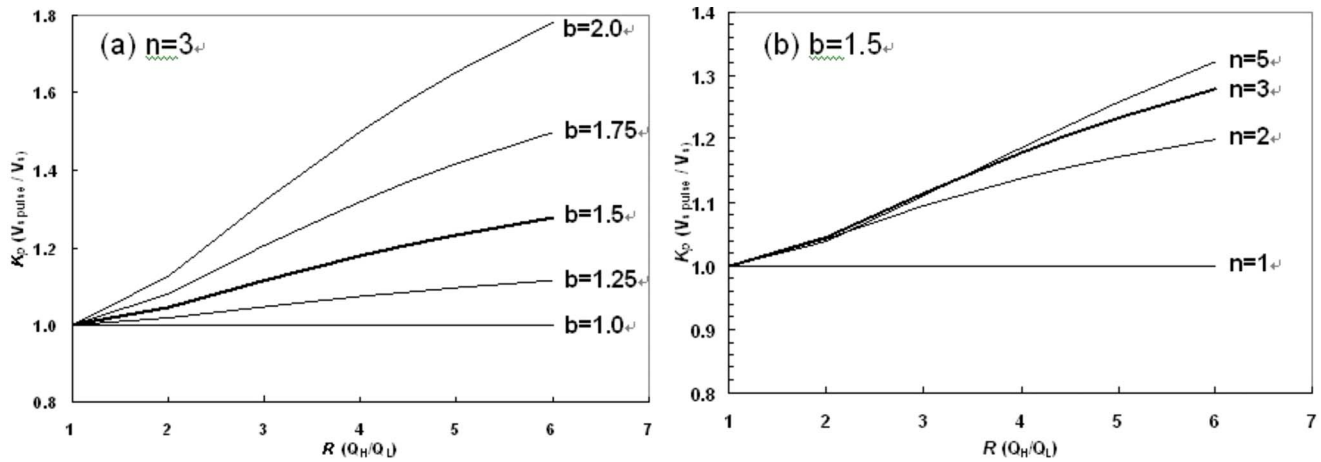


Fig. 14. Variation of K_p for (a) different values of b at $n=3$; (b) different n values at $b=1.5$

bed channel with narrower channels and vegetated point bars. This lower reach may also remain an important source for sand mining that may also have an impact on the river morphology in the coming years.

Summary and Conclusions

The effects of flow pulses on hydraulic geometry are examined over a 45-km reach of the Hwang River between the Hapcheon Reregulation Dam and the confluence with the Nakdong River. During the postdam period (1989–2005) the peak flows decreased to 19.3% of predam conditions and the sediment supply was essentially eliminated. Historical time series data such as flow rate, aerial photos, cross section surveys, sediment transport, and bed-material data were analyzed. A theoretical analysis of the effects of flow pulses led to the determination of the sediment pulsing coefficient K_p which is presented in Eq. (7). The coefficient describes the ratio of sediment transport for flow pulses in comparison with steady flow. The coefficient is tested with steady flow sediment transport for the 45-km reach of the Hwang River below Hapcheon Dam from 1983 to 2003. The primary conclusions are as follows:

1. The effect of flow pulses is examined and the sediment pulsing coefficient K_p in Eq. (7) defines the increase in sediment transport due to flow pulse. The unsteady flow effects become nonnegligible (greater than 10% difference or $K_p > 1.1$) when the ratio of high to low flow discharge is greater than 3. On the Hwang River, the sediment transport rate (t/day) of daily pulses is about 20% larger than for average daily flow.
 2. The channel bed material armored from sand to gravel (from 2.16 to 44 mm) over the 5-km reach below the reregulation dam. The river channel bed elevation degraded an average of 2.6 m over the 20-km reach downstream of the reregulation dam. The channel width also decreased by about 50% after dam construction.
 3. The numerical results with a calibrated GSTAR-1D model predict armoring and a maximum channel scour depth as high as 4 m (RMS error < 1 m). The channel degradation should extend about 20 km downstream from the reregulation dam. Also, the thalweg elevation is predicted to become relatively stable after 2013.
- The numerical model results are based on a limited compari-

son of steady and unsteady flow models. The effects of unsteady flow become more significant as K_p increases. Future research improvements may include more comprehensive comparisons of steady versus unsteady model results as well as a better understanding of sediment transport in unsteady flows.

Acknowledgments

This paper is primarily the result of the analysis of the first writer during his Ph.D. studies at Colorado State University. Financial support from the Korea Water Resources Corporation (K-water) during the course of the study is gratefully acknowledged. However, the results do not necessarily reflect policies or endorsement of K-water. The writers are grateful to Hyosub Cho, Jungyup Kim, and Changrae Jang and Jahun Jun at K-water who individually contributed to this study. We finally appreciate the helpful comments of the anonymous reviewers and the editorial board of the journal.

Notation

The following symbols are used in this paper:

- a = coefficient of the sediment rating curve;
- b = exponent of sediment rating curve;
- K_p = sediment pulsing coefficient describing the ratio of the sediment volume transported by a flow pulse compared to the sediment volume transported by the same volume of fluid under steady flow;
- n = Manning's resistance coefficient;
- n = duration of the flow pulse;
- Q_H = peak pulse flow discharge (L^3/T);
- Q_L = minimum pulse flow discharge (L^3/T);
- Q_s = sediment discharge (L^3/T);
- \bar{Q} = average pulse flow discharge (L^3/T);
- r = Q_H/Q_L discharge ratio for the pulse;
- T = period of time for the sediment load calculation;
- \bar{V}_s = sediment volume transported under steady flow (L^3); and
- $V_{s, pulse}$ = sediment volume transported by the flow pulse (L^3).

References

- Ackers, P., and White, W. R. (1973). "Sediment transport: New approach and analysis." *J. Hydr. Div.*, 99(HY11), 2041–2060.
- Brandt, S. A. (2000). "Classification of geomorphological effects downstream of dams." *Catena*, 40, 375–401.
- Chang, H. H. (2006). *Fluvial-12 mathematical model for erodible channels; users manual*, Chang Consultants, Rancho Santa Fe, Calif.
- Choi, S. U., Yoon, B., Woo, H., and Cho, K. (2004). "Effect of flow regime changes due to damming on the river morphology and vegetation cover in the downstream river reach: A case of Hapcheon Dam on the Hwang River." *J. Korea Water Resources Association*, 37(1), 55–66 (in Korean).
- Downs, P. W., and Gregory, K. J. (2004). *River channel management: Towards sustainable catchment hydrosystems*, Oxford University Press, Oakland, Calif.
- Engelund, F., and Hansen, E. (1972). *A monograph on sediment transport in alluvial streams*, Teknisk Forlag, Copenhagen, Denmark.
- Ferguson, R. I. (1986). "Hydraulics and hydraulic geometry." *Prog. Phys. Geogr.*, 10, 1–31.
- Food and Agriculture Organization of the United Nations (FAO) and Korea Water Resources Development Corporation (KOWACO). (1971). "Pre-investment survey of the Nakdong River Basin, Korea." *Sediment transportation in rivers of the Nakdong basin*, Vol. 4, FAO and KOWACO, Rome, Italy and Daejeon, Korea.
- Grant, G. E., Schmidt, J. C., and Lewis, S. L. (2003). "A geological framework for interpreting downstream effects of dams on rivers." *Water Sci. Appl.*, 7, 209–225.
- Gregory, K. J., and Park, C. (1974). "Adjustment of river channel capacity downstream from a reservoir." *Water Resour. Res.*, 10(4), 870–873.
- Greimann, B. P., and Huang, J. (2006). *One-dimensional modeling of incision through reservoir deposits*, Sedimentation and River Hydraulics Group, Technical Service Center, Bureau of Reclamation, Denver Federal Center, Denver.
- Hey, R. D. (1979). "Dynamic process—Response model of river channel development." *Earth Surf. Processes Landforms*, 4, 59–72.
- Huang, H. Q., and Nanson, G. C. (2000). "Hydraulic geometry and maximum flow efficiency as products of the principle of least action." *Earth Surf. Processes Landforms*, 25, 1–16.
- Huang, J. V., and Greimann, B. P. (2006). *Draft user's manual for GSTAR-ID 1.1.4, generalized sediment transport for alluvial rivers—One dimension, version 1.1.4*, U.S. Dept. of Interior, Bureau of Reclamation, Technical Service Center, Sedimentation and River Hydraulics Group, Denver Federal Center, Denver.
- Huang, J. V., Greimann, B. P., and Bauer, T. (2006). *Development and application of GSTAR-ID*, Sedimentation and River Hydraulics Group, Technical Service Center, Bureau of Reclamation, Denver Federal Center, Denver.
- Julien, P. Y. (2002). *River mechanics*, Cambridge University Press, New York.
- Knighton, A. D. (1998). *Fluvial forms and processes: A new perspective*, Oxford University Press, New York.
- Korea Water Resources Development Corporation (KOWACO). (2002). *The report of survey of reservoir sediment deposition of Hapcheon Dam*, Daejeon, Korea (in Korean).
- Lamberti, A. (1992). "Dynamic and variational approaches to the river regime relation." *Entropy and energy dissipation in water resources*, V. P. Singh and M. Fiorentino, eds., Kluwer, Dordrecht, The Netherlands, 507–525.
- Lane, E. W. (1955). "The importance of fluvial morphology in hydraulic engineering." *Proc., ASCE*, Vol. 81, ASCE, Reston, Va., 62–79.
- Langendoen, E. J. (2000). "CONCEPTS—Conservational channel evolution and pollutant transport system." *Research Rep. No. 16*, USDA-ARS National Sedimentation Laboratory, Washington, D.C.
- Leon, C., Julien, P. J., and Baird, D. C. (2009). "Equivalent widths of the middle Rio Grande, New Mexico." *J. Hydraul. Eng.*, 135(4), 306–315.
- Miller, T. K. (1991a). "A model of stream channel adjustment: Assessment of Rubey's hypothesis." *J. Geol.*, 99, 699–710.
- Miller, T. K. (1991b). "An assessment of the equable change principle in at-a-station hydraulic geometry." *Water Resour. Res.*, 27, 2751–2758.
- Ministry of Construction and Transportation (MOCT) of Korea. (1983). "A report of master plan for the river improvement project in the Hwang River, Nakdong River basin." *Rep. Prepared for MOCT of Korea*, Korean Government (in Korean).
- Ministry of Construction and Transportation (MOCT) of Korea. (1993). "A report of analysis for the river bed change in the Hwang River, Nakdong River basin." *Rep. Prepared for MOCT of Korea*, Korean Government (in Korean).
- Ministry of Construction and Transportation (MOCT) of Korea. (2003). "A report of master plan for the river improvement project in the Hwang River, Nakdong River basin." *Rep. Prepared for MOCT of Korea*, Korean Government (in Korean).
- Molinas, A., and Yang, C. T. (1986). *Computer program user's manual for GSTARS (Generalized stream tube model for alluvial river simulation)*, U.S. Dept. of Interior, Bureau of Reclamation, Technical Service Center, Denver Federal Center, Denver.
- Page, K., Read, A., Frazier, P., and Mount, N. (2005). "The effect of altered flow regime on the frequency and duration of bankfull discharge: Murrumbidgee River, Australia." *River Res. Appl.*, 21, 567–578.
- Phillips, J. D., Slattery, M. C., and Musselman, Z. A. (2005). "Channel adjustment of the lower Trinity River, Texas, downstream of Livingston Dam." *Earth Surf. Processes Landforms*, 30, 1419–1439.
- Richard, G. A., and Julien, P. Y. (2005). "Statistical analysis of lateral migration of the Rio Grande, New Mexico." *Geomorphology*, 71, 139–155.
- Richard, G. A., Julien, P. Y., and Baird, D. C. (2005). "Case study: Modeling the lateral mobility of the Rio Grande below Cochiti Dam, New Mexico." *J. Hydraul. Eng.*, 131(11), 931–941.
- Schumm, S. A. (1985). "Pattern of alluvial rivers." *Annu. Rev. Earth Planet Sci.*, 13, 5–27.
- Shin, Y. H. (2007). "Channel changes downstream of the Hapcheon Regulation Dam in South Korea." Ph.D. dissertation, Colorado State Univ., Fort Collins, Colo.
- Simon, A., Thomas, R. E., Curini, A., and Shields, F. D., Jr. (2002). "Case study: Channel stability of the Missouri River, Eastern Montana." *J. Hydraul. Eng.*, 10, 880–890.
- Simon, A., and Thorne, C. R. (1996). "Channel adjustment of an unstable coarse-grained stream: Opposing trends of boundary and critical shear stress, and the applicability to extremal hypotheses." *Earth Surf. Processes Landforms*, 21, 155–180.
- Tetra Tech, Inc. (2001). "EFDC1D, a one dimensional hydrodynamic and sediment transport model for river and stream networks, model theory and users guide." *Rep. Prepared for U.S. EPA*, Office of Science and Technology, Washington, D.C.
- U.S. Army Corps of Engineers. (1993). *HEC-6 scour and deposition in rivers and reservoirs; user's manual*, The Hydraulic Engineering Center, Vicksburg, Miss.
- U.S. Department of Interior, Bureau of Reclamation (USBR). (2006). *Draft user's manual for GSTAR-ID 1.1.3*, Sedimentation and River Hydraulic Group, USBR Technical Service Center Sedimentation and River Hydraulic Group, Denver.
- van Rijn, L. C. (1984). "Sediment transport. Part I: Bed load transport." *J. Hydraul. Eng.*, 110(10), 1431–1456.
- Williams, G. P., and Wolman, M. G. (1984). "Downstream effects of dams on alluvial rivers." *U.S. Geol. Surv. Prof. Pap.*, 1286, 7–14.
- Woo, H., Choi, S. U., and Yoon, B. (2004a). "Downstream effect of dam on river morphology and sandbar vegetation." *Proc., Symp. of the 72nd Annual ICOLD Meeting*, ICOLD.
- Woo, H., Lee, D. S., Ahn, H. K., and Lee, C. S. (2004b). "Effect of river

- channel meander on hydro-geomorphologically induced vegetation expansion on sandbars." *Proc., 6th ICHE*.
- Wu, W., and Vieira, D. A. (2002). "One-dimensional channel network model CCHE1D version 3.0—Technical manual." *Technical Rep. No. NCCHE-TR-2002-1*, National Center for Computational Hydroscience and Engineering, The Univ. of Mississippi, Oxford, Miss.
- Yang, C. T. (1973). "Incipient motion and sediment transport." *J. Hydraul. Eng.*, 99(HY10), 1679–1704.
- Yang, C. T. (1979). "Unit stream power equation for gravel." *J. Hydraul. Eng.*, 40, 123–138.
- Yang, C. T. (1992). "Force, energy, entropy, and energy dissipation rate." *Entropy and energy dissipation in water resources*, V. P. Singh and M. Fiorentino, eds., Kluwer, Dordrecht, The Netherlands, 63–89.
- Yang, C. T., and Simões, F. J. M. (2000). *User's manual for GSTARS 2.1 (generalized stream tube model for alluvial river simulation version 2.1)*, U.S. Bureau of Reclamation, Technical Service Center, Denver Federal Center, Denver.
- Yang, C. T., and Simões, F. J. M. (2002). *User's manual for GSTAR3 (generalized stream tube model for alluvial river simulation version 3.0)*, U.S. Bureau of Reclamation, Technical Service Center, Denver Federal Center, Denver.